RSC Advances

This is an *Accepted Manuscript*, which has been through the Royal Society of Chemistry peer review process and has been accepted for publication.

Accepted Manuscripts are published online shortly after acceptance, before technical editing, formatting and proof reading. Using this free service, authors can make their results available to the community, in citable form, before we publish the edited article. This *Accepted Manuscript* will be replaced by the edited, formatted and paginated article as soon as this is available.

You can find more information about *Accepted Manuscripts* in the Information for Authors.

Please note that technical editing may introduce minor changes to the text and/or graphics, which may alter content. The journal's standard Terms & Conditions and the Ethical guidelines still apply. In no event shall the Royal Society of Chemistry be held responsible for any errors or omissions in this *Accepted Manuscript* or any consequences arising from the use of any information it contains.

ROYAL SOCIETY OF CHEMISTRY

www.rsc.org/advances

Graphical contents entry:

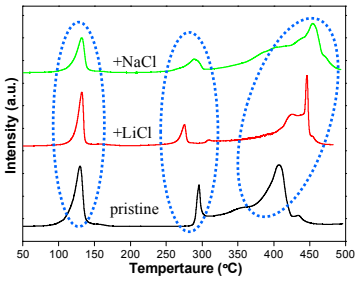

The presence of NaCl and LiCl changes the dehydrogenation/hydrogenation kinetics of the $6LiBH_4$-$Mg(AlH_4)_2$ composite.

RSC Advances Accepted Manuscript

RSC Advances RSCPublishing

PAPER

Cite this: DOI: 10.1039/x0xx00000x

Received 00th January 2012,
Accepted 00th January 2012

DOI: 10.1039/x0xx00000x

www.rsc.org/

New insights into the effects of NaCl and LiCl on the hydrogen storage behaviours of a $6LiBH_4$-$Mg(AlH_4)_2$ composite

Yuepeng Pang[a,b], Yongfeng Liu[a]*, Xin Zhang[a], You Li[a], Mingxia Gao[a], Hongge Pan[a]

The effects of the NaCl and LiCl by-products generated during the synthesis of $Mg(AlH_4)_2$ on the hydrogen storage properties of a $6LiBH_4$-$Mg(AlH_4)_2$ composite are investigated and clarified for the first time. The results indicate that the presence of NaCl and LiCl changes the dehydrogenation/hydrogenation kinetics of the $6LiBH_4$-$Mg(AlH_4)_2$ composite in addition to producing a distinct reduction in the hydrogen capacity. For the NaCl-containing sample, the chemical composition is changed due to the metathesis reaction between NaCl and $LiBH_4$ during ball milling, which converts the NaCl and $LiBH_4$ to LiCl and $NaBH_4$. However, for the LiCl-containing system, the kinetic barriers of the dehydrogenation reaction were changed by the presence of LiCl, which is responsible for the change in the dehydrogenation temperature. These findings elucidate the effects of NaCl and LiCl, which are produced during the synthesis of $Mg(AlH_4)_2$, on the hydrogen storage behaviours of the $6LiBH_4$-$Mg(AlH_4)_2$ composite.

Introduction

The greatest challenge for the widespread use of hydrogen energy is how to store it in a safe, efficient and reversible manner.[1,2] Compared to high pressure compression and liquefaction via cryogenics, storing hydrogen in solid state materials has potential advantages in terms of the volumetric density and safety, especially for mobile applications.[1-3] Since Bogdanović and co-worker demonstrated that reversible hydrogen storage in $NaAlH_4$ can be achieved at moderate temperature and hydrogen pressure by the addition of Ti-based catalysts in 1997, more and more attention has been paid to light-metal complex hydrides, including metal alanates and borohydrides, as promising hydrogen storage candidates due to their high gravimetric and volumetric hydrogen capacities.[3-6]

$Mg(AlH_4)_2$ has a high theoretical hydrogen capacity of 9.3 wt% (on material basis[7,8], similarly hereinafter), and approximately 7 wt% of hydrogen can be released below 180 °C according to the following reaction:[9]

$$Mg(AlH_4)_2 \rightarrow MgH_2+2Al+3H_2 \quad (1)$$

Unfortunately, hydrogen desorption from reaction (1) is mildly exothermic in nature. It is therefore difficult for the $Mg(AlH_4)_2$ to be re-hydrogenated under moderate conditions, which is the key disadvantage of $Mg(AlH_4)_2$ as a reversible hydrogen storage material.[10,11]

As a typical borohydride, $LiBH_4$ delivers a hydrogen capacity as high as 13.8 wt% via reaction (2).[12]

$$LiBH_4 \leftrightarrow LiH+B+\frac{3}{2}H_2 \quad (2)$$

However, reaction (2) proceeds at a rather high temperature above 400 °C due to the problematic thermodynamics with an enthalpy change of approximately 74 kJ/mol-H_2.[13] In particular, the reverse of reaction (2) requires even harsher conditions of 600 °C and 150 atm of hydrogen pressure.[14] These prevent $LiBH_4$ from having practical applications as a hydrogen storage material.

Recently, a new strategy was proposed to tailor the thermodynamics of the dehydrogenation reactions of complex hydrides by forming a reactive composite with metals or metal hydrides. A successful example is the $2LiBH_4$-MgH_2 reactive hydride composite developed by Vajo *et al.*[15] It was reported that the dehydrogenation temperature was reduced by 250 °C because of the formation of MgB_2. More attractively, the dehydrogenation product can be re-hydrogenated at 350 °C and 100 bar of hydrogen, which are more moderate conditions relative to those required for the pristine $LiBH_4$. After that, a variety of reactive hydride composites have been investigated and developed, such as $LiBH_4$-Mg(Al), $LiBH_4$-CaH_2, $LiBH_4$-ScH_2, $LiBH_4$-$LiAlH_4$, $LiBH_4$-$NaAlH_4$, $LiBH_4$-$Mg(AlH_4)_2$, $LiBH_4$-$Ca(AlH_4)_2$, $NaBH_4$-$LiAlH_4$, $Mg(BH_4)_2$-$LiAlH_4$, $Mg(BH_4)_2$-$NaAlH_4$, and so on.[16-23] Among these studied materials, the $6LiBH_4$-$Mg(AlH_4)_2$ composite exhibited a significantly lower dehydrogenation temperature, faster kinetics and better reversibility than the MgH_2- or Al-$LiBH_4$ individually.[19] It was reported that the $6LiBH_4$-$Mg(AlH_4)_2$ composite released 11.8 wt% of hydrogen

RSC Advances Accepted Manuscript

within 200 min at 400 ºC, and the dehydrogenated sample absorbed 6.4 wt% of hydrogen within 300 min at 400 ºC. Here, it should be mentioned that $Mg(AlH_4)_2$ was synthesised by a mechanochemically activated metathesis reaction of $LiAlH_4$ and $MgCl_2$ without solvent, and the by-product LiCl was not removed, which induces a distinct reduction in the practical hydrogen capacity due to the dead weight. Moreover, several recent studies revealed that the chlorides may play important roles for hydrogen desorption from complex hydrides instead of being only inert species.[24-26] Singh *et al*[24] reported that NaCl acted as the nucleation centre of NaH in $TiCl_3$-doped $NaAlH_4$ and thus accelerated the decomposition of Na_3AlH_6. A similar phenomenon was also observed in the TiF_4-doped Na_2LiAlH_6.[25] More recently, it was found that adding a small amount of lithium halides (LiCl, LiBr, and LiI) significantly improved the hydrogen storage properties of the $LiNH_2$-MgH_2 composite by forming fast Li-ion conductors.[26] Consequently, a question raised is what is the real role played by the NaCl and LiCl by-products in the dehydrogenation/hydrogenation of the $6LiBH_4$-$Mg(AlH_4)_2$ composite.

In this work, the effects of NaCl and LiCl on the dehydrogenation/hydrogenation of the $6LiBH_4$-$Mg(AlH_4)_2$ composite were studied and systematically compared for the first time. The results showed that NaCl could react with $LiBH_4$ to form LiCl and $NaBH_4$ during ball milling, which changes the chemical composition of the $6LiBH_4$-$Mg(AlH_4)_2$ composite. As for LiCl, its presence affected the hydrogen desorption/absorption kinetics of the $6LiBH_4$-$Mg(AlH_4)_2$ composite even though it does not react with $LiBH_4$ or $Mg(AlH_4)_2$ during the ball milling and heating processes. These findings indicate that there is a distinct effect from the NaCl and LiCl by-products generated during the synthesis of $Mg(AlH_4)_2$ on the hydrogen storage properties of the $6LiBH_4$-$Mg(AlH_4)_2$ composite, which elucidates the roles played by NaCl and LiCl.

Experimental

The commercial chemicals $NaAlH_4$ (ACROS, 93%), $LiAlH_4$ (Alfa Aesar, 97%), $MgCl_2$ (Alfa Aesar, 99%) and $LiBH_4$ (Sigma-Aldrich, 95%) were used as received without further purification. Pure $Mg(AlH_4)_2$ was synthesised by the method described in our previous work.[27] The $6LiBH_4$-$Mg(AlH_4)_2$ composite was obtained by first ball milling $Mg(AlH_4)_2$ for 3 h and then ball milling the as-milled $Mg(AlH_4)_2$ with $LiBH_4$ for 12 h. Ball milling was carried out on a planetary ball mill (QM-3SP4, Nanjing) rotated at 500 rpm. The ball-to-sample weight ratio was approximately 60:1. The mill was set to rotate for 0.2 h in one direction and then rotate in the reverse direction after a 0.1 h pause. For comparison, the $6LiBH_4$-$Mg(AlH_4)_2$-2LiCl and $6LiBH_4$-$Mg(AlH_4)_2$-2NaCl composites were also prepared by means of a two-step method. First, the $Mg(AlH_4)_2$-2LiCl and $Mg(AlH_4)_2$-2NaCl composites were produced by ball milling $LiAlH_4$ with $MgCl_2$ or $NaAlH_4$ with $MgCl_2$ for 3 h. Then, the $6LiBH_4$-$Mg(AlH_4)_2$-2LiCl and $6LiBH_4$-$Mg(AlH_4)_2$-2NaCl composites were obtained after ball milling the as-prepared $Mg(AlH_4)_2$-2LiCl and $Mg(AlH_4)_2$-2NaCl composites with $LiBH_4$ for 12 h, respectively. All of the sample handing was performed in a glove box (MBRAUN, Germany) filled with pure argon (H_2O, O_2 < 1 ppm).

The temperature dependence of hydrogen desorption from the samples was measured using a homemade temperature-programmed desorption (TPD) system with an online mass spectrometer (Hiden QIC-20, England). Approximately 60 mg of sample was loaded into a stainless steel microreactor and gradually heated from room temperature to 500 °C at a rate of 2 °C/min with a continuous flow of pure Ar as the carrier gas. The quantitative dehydrogenation/hydrogenation performances were determined by a volumetric method using a Sieverts-type apparatus. The pressure and temperature in the reactor and gas reservoir were monitored and recorded automatically. The quantities of hydrogen desorbed/absorbed were determined by calculating the pressure and temperature changes in the reactor using the equation of state. The heat effect of hydrogen desorption was determined by differential scanning calorimetry (DSC) on a Netzsch DSC 200 F3 unit (Germany). Pure Ar was used as the carrier gas, and the heating rate was set to 10 °C/min.

The phase structures of the samples were characterised by an X'pert PRO diffractometer (PANalytical, The Netherland) with Cu-K_α radiation at 40 kV and 40 mA. The XRD data were collected in the 2θ range of 10-90° at room temperature. A homemade container was applied to protect the powdery samples from air and moisture contamination during transfer and scanning. Fourier transform infrared (FTIR) spectra were acquired using a Bruker Tensor 27 unit (Germany) in the transmission mode. The sample being tested was prepared by cold-pressing a mixture of the target powder and KBr (Alfa Aesar, 99%) at a weight ratio of 200:1.

Results and discussion

Fig. 1 shows the FTIR spectra and XRD patterns of the as-prepared $6LiBH_4$-$Mg(AlH_4)_2$, $6LiBH_4$-$Mg(AlH_4)_2$-2LiCl and $6LiBH_4$-$Mg(AlH_4)_2$-2NaCl composites. As shown in Fig. 1a, it can be observed that the three composites with and without LiCl and NaCl exhibited identical FTIR spectra as the B-H vibrations at 2386, 2291, 2223 and 1125 cm^{-1} and Al-H vibrations at 1830 cm^{-1} were clearly observed. Further XRD examinations revealed that the characteristic reflections of $LiBH_4$ and $Mg(AlH_4)_2$ dominated the XRD profiles of all three of the composites (Fig. 1b). For the $6LiBH_4$-$Mg(AlH_4)_2$-2LiCl composite, the typical diffraction peaks of LiCl were also unambiguously detected with considerable intensities. Therefore, we believe that the $6LiBH_4$-$Mg(AlH_4)_2$ and $6LiBH_4$-$Mg(AlH_4)_2$-2LiCl composites are only the physical mixtures of the corresponding chemicals after ball milling at room temperature. In other words, no chemical reaction occurred between $LiBH_4$, $Mg(AlH_4)_2$ and LiCl during ball milling. However, NaCl is invisible in the $6LiBH_4$-$Mg(AlH_4)_2$-2NaCl composite, and two new phases of LiCl and $NaBH_4$ were identified in addition to the $LiBH_4$ and $Mg(AlH_4)_2$. This result suggests that NaCl reacts with $LiBH_4$ and is converted to LiCl and $NaBH_4$ during ball milling as described by the following reaction:

$$LiBH_4 + NaCl \xrightarrow{BM} NaBH_4 + LiCl \quad (3)$$

RSC Advances Accepted Manuscript

 This journal is © The Royal Society of Chemistry 2012

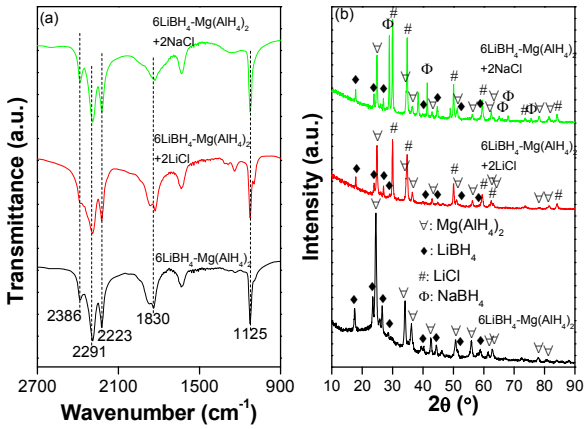

Fig. 1 FTIR spectra (a) and XRD patterns (b) of the $6LiBH_4$-$Mg(AlH_4)_2$ composite with and without LiCl and NaCl.

It is known that the standard enthalpies of formation of $LiBH_4$, NaCl, $NaBH_4$, and LiCl are -190.799, -411.120, -408.266, and -191.841 kJ/mol, and their standard entropies are 75.902, 72.132, 59.300, and 101.391 J/mol, respectively.[28] Thus, the Gibbs free energy change of reaction (3) was determined to be –1.99 kJ/mol (27 °C), which indicates that the metathesis reaction between $LiBH_4$ and NaCl is thermodynamically favourable, which can be initialised by the collision of grinding balls during energetic ball-milling. As a result, the $6LiBH_4$-$Mg(AlH_4)_2$-2NaCl composite converted to $4LiBH_4$-$2NaBH_4$-$Mg(AlH_4)_2$-2LiCl after ball milling.

Hydrogen desorption properties of the as-prepared $6LiBH_4$-$Mg(AlH_4)_2$ composites with and without LiCl and NaCl were measured as a function of temperature by TPD and volumetric methods. Fig. 2 shows the TPD curves of the as-prepared $6LiBH_4$-$Mg(AlH_4)_2$, $6LiBH_4$-$Mg(AlH_4)_2$-2LiCl and $6LiBH_4$-$Mg(AlH_4)_2$-2NaCl composites. It is observed that the as-prepared $6LiBH_4$-$Mg(AlH_4)_2$ composite roughly exhibits a four-step dehydrogenation behaviour in the tested temperature range. The four hydrogen desorption peaks appeared at 130, 295, 407 and 435 °C as the temperature was increased. For the $6LiBH_4$-$Mg(AlH_4)_2$-2LiCl and $6LiBH_4$-$Mg(AlH_4)_2$-2NaCl composites, the first peak of dehydrogenation remains at 130 ºC, and the second dehydrogenation step exhibits a shift to a lower temperature relative to the $6LiBH_4$-$Mg(AlH_4)_2$ composite. More interestingly, the dehydrogenation

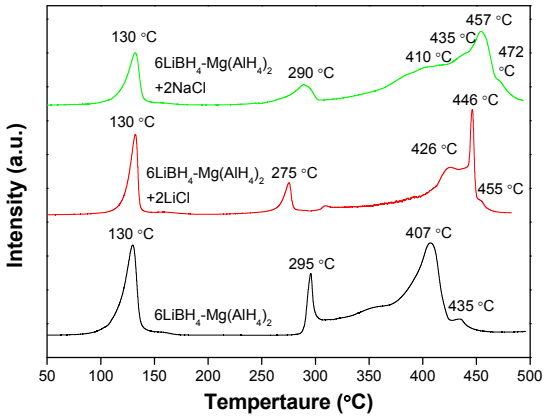

Fig. 2 TPD curves of the $6LiBH_4$-$Mg(AlH_4)_2$ composite with and without LiCl and NaCl.

Table 1 The amount of hydrogen desorbed from the $6LiBH_4$-$Mg(AlH_4)_2$ composite with and without LiCl and NaCl.

Samples	Hydrogen desorption amount (wt%)				
	1st step	2nd step	3rd step	4th step	total
$6LiBH_4$-$Mg(AlH_4)_2$	2.6	0.9	8.0	0.3	11.8
$6LiBH_4$-$Mg(AlH_4)_2$-2LiCl	1.9	0.7	5.9	0.2	8.7
$6LiBH_4$-$Mg(AlH_4)_2$-2NaCl	1.8	0.6	5.1	0.2	7.7

behaviours of $6LiBH_4$-$Mg(AlH_4)_2$-2LiCl and $6LiBH_4$-$Mg(AlH_4)_2$-2NaCl become more complicated above 350 ºC. It is observed that at above 350 ºC, the $6LiBH_4$-$Mg(AlH_4)_2$-2LiCl composite exhibits three dehydrogenation peaks, and there are four peaks for the $6LiBH_4$-$Mg(AlH_4)_2$-2NaCl composite above 350 °C. It is noteworthy that the temperatures of these dehydrogenation peaks are distinctly higher than those of the halide-free sample. Therefore, we believe that the presence of LiCl and NaCl affects the dehydrogenation behaviour of the $6LiBH_4$-$Mg(AlH_4)_2$ composite. This conjecture is further confirmed by the volumetric release measurements. As shown in Fig. 3, a slight shift to a lower temperature was detected for the second dehydrogenation step of the $6LiBH_4$-$Mg(AlH_4)_2$-2LiCl and $6LiBH_4$-$Mg(AlH_4)_2$-2NaCl composites. However, a shift to a higher temperature was observed for the third and fourth dehydrogenation steps. This is in excellent agreement with the TPD results. Quantitative analyses revealed that the $6LiBH_4$-$Mg(AlH_4)_2$ composite delivered 2.6, 0.9, 8.0 and 0.3 wt% hydrogen at 70-150 °C, 250-300 °C, 300-420 °C and 420-500 °C as shown in Table 1. The total dehydrogenation amounted to 11.8 wt%, which is very close to the theoretical hydrogen capacity of 12.4 wt%. For the $6LiBH_4$-$Mg(AlH_4)_2$-2LiCl composite, the dehydrogenation amounts of the four steps were calculated to be 1.9, 0.7, 5.9 and 0.2 wt% at 106-160 °C, 220-290 ºC, 290-450 °C and 450-500 ºC, respectively, and the dehydrogenation amounts were 1.8, 0.6, 5.1 and 0.2 wt% of hydrogen at 100-160 ºC, 220-290 ºC, 290-480 °C and 480-500 ºC for the $6LiBH_4$-$Mg(AlH_4)_2$-2NaCl composite. The total dehydrogenation amounts were determined to be 8.7 wt% and 7.7 wt% for the $6LiBH_4$-$Mg(AlH_4)_2$-2LiCl and $6LiBH_4$-$Mg(AlH_4)_2$-2NaCl composites, respectively. Specifically, the practical hydrogen

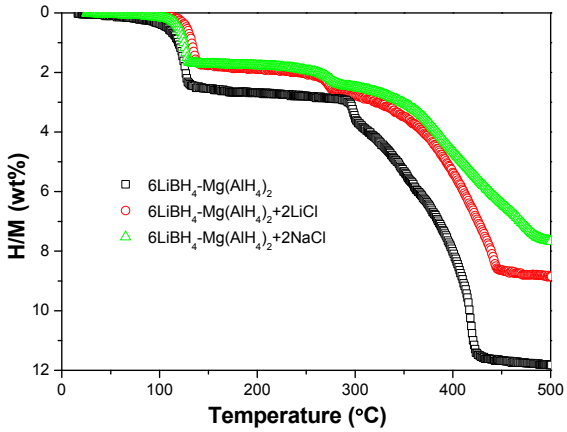

Fig. 3 Volumetric release curves of the $6LiBH_4$-$Mg(AlH_4)_2$ composite with and without LiCl and NaCl.

RSC Advances Accepted Manuscript

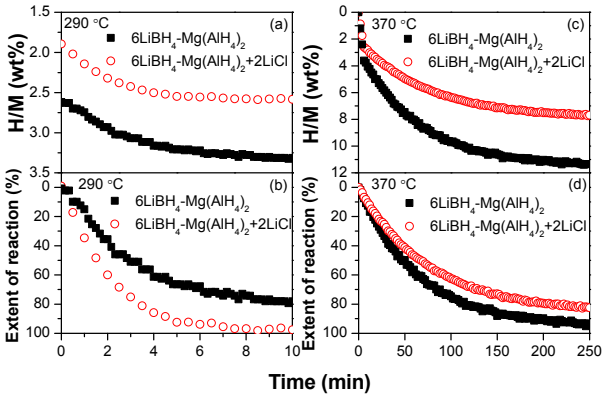

Fig. 4 Isothermal dehydrogenation curves of the $6LiBH_4$-$Mg(AlH_4)_2$ composite with and without LiCl at 290 (a, b) and 370 °C (c, d). The weight percent (a, c) and the extent of reaction (b, d) are used as the y axis variables

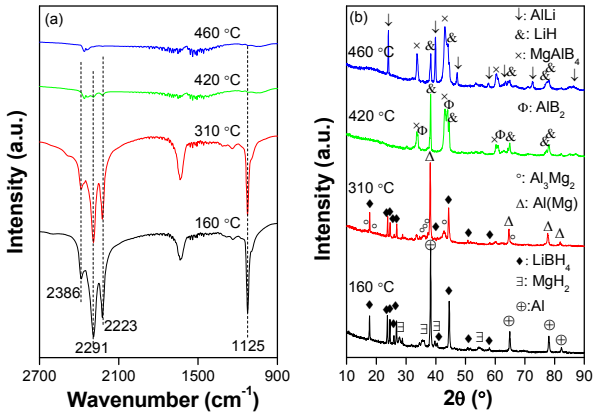

Fig. 5 FTIR spectra (a) and XRD patterns (b) of the $6LiBH_4$-$Mg(AlH_4)_2$ composite dehydrogenated at different temperatures.

capacity was distinctly reduced because no hydrogen atoms were included in LiCl and NaCl. In addition, it should be noted that the $6LiBH_4$-$Mg(AlH_4)_2$-2NaCl composite exhibited the lowest hydrogen capacity and much higher dehydrogenation temperatures for the third and fourth steps among the three studied samples. This can be attributed to the larger molar weight of NaCl than that of LiCl and the formation of $NaBH_4$ caused by the metathesis reaction between $LiBH_4$ and NaCl because $NaBH_4$ is more thermodynamically stable than $LiBH_4$ leading to dehydrogenation occurring at higher temperatures as extensively reported previously.[3] Because NaCl is converted to LiCl after ball milling, the follow-up in-depth investigations on the hydrogen storage thermodynamics and kinetics were concentrated on $6LiBH_4$-$Mg(AlH_4)_2$-2LiCl.

Fig. 4 presents the isothermal dehydrogenation curves of the $6LiBH_4$-$Mg(AlH_4)_2$ and $6LiBH_4$-$Mg(AlH_4)_2$-2LiCl composites. It is observed that approximately 3.3 and 2.6 wt% of hydrogen were quickly released from the $6LiBH_4$-$Mg(AlH_4)_2$ and $6LiBH_4$-$Mg(AlH_4)_2$-2LiCl composites, respectively, within 10 min at 290 °C. Such dehydrogenation amounts are close to the capacities of the initial two steps of dehydrogenation. To compare the dehydrogenation kinetics, the isothermal dehydrogenation curves were re-plotted by calculating the extent of reaction as shown in Fig. 4b. It is clear that a faster dehydrogenation rate was observed for the $6LiBH_4$-$Mg(AlH_4)_2$-2LiCl composite in comparison with the $6LiBH_4$-$Mg(AlH_4)_2$ composite, indicating that the presence of LiCl improves the dehydrogenation kinetics of the $6LiBH_4$-$Mg(AlH_4)_2$ composite at low temperatures. When the dehydrogenation temperature was elevated to 370 °C, hydrogen desorption amounts increased to 11.3 wt% and 7.7 wt% for the $6LiBH_4$-$Mg(AlH_4)_2$ and $6LiBH_4$-$Mg(AlH_4)_2$-2LiCl composites, respectively, within 250 min (Fig. 4c). Re-plotting the isothermal dehydrogenation curves by using the extent of reaction against time (Fig. 4d) shows a slightly slower overall dehydrogenation rate for the LiCl-containing composite, which can be attributed to that the majority of dehydrogenation occurred at higher temperatures for the $6LiBH_4$-$Mg(AlH_4)_2$-2LiCl composite as shown in Fig. 3. These results indicate that the presence of LiCl accelerates the dehydrogenation rate of the second step of the $6LiBH_4$-$Mg(AlH_4)_2$ composite but retards the dehydrogenation rate of the third step, which is consistent with the non-isothermal results (Fig. 2 and 3).

To understand the chemical events occurring in the hydrogen desorption process, FTIR and XRD examinations were carried out on the dehydrogenated $6LiBH_4$-$Mg(AlH_4)_2$ and $6LiBH_4$-$Mg(AlH_4)_2$-2LiCl samples at different temperatures. Fig. 5 presents the results of the FTIR and XRD measurements of the $6LiBH_4$-$Mg(AlH_4)_2$ composite. FTIR analyses (Fig. 5a) reveal that after dehydrogenation at 160 and 310 °C, only the absorbances of the B-H vibration were observed, and the Al-H vibration was invisible. When the samples were dehydrogenated at 420 and 460 °C, no apparent absorbance was detected in the FTIR spectrum, indicating the disappearance of the B-H vibration due to the consumption of $LiBH_4$. In a further XRD experiment (Fig. 5b), the reflections of MgH_2 and Al were identified along with the absence of $Mg(AlH_4)_2$ after dehydrogenation at 160 °C. When the sample was heated to 310 °C, the newly developed MgH_2 and Al disappeared, and an Al(Mg) solid solution phase and Al_3Mg_2 were discernible. At 420 °C, $LiBH_4$, Al_3Mg_2 and the Al(Mg) solid solution were completely consumed while LiH, AlB_2 and $MgAlB_4$ were formed. When the temperature was further increased to 460 °C, LiAl, LiH and $MgAlB_4$ are the only three phases detected in the dehydrogenated sample. According to the above discussion, we believe that upon heating, $Mg(AlH_4)_2$ in the $6LiBH_4$-$Mg(AlH_4)_2$ composite first decomposes to form MgH_2, Al and H_2. Then, MgH_2 reacts with Al to form the Al(Mg) solid solution, Al_3Mg_2 and H_2 as the temperature is increased. After that, the chemical reaction between $LiBH_4$, the Al(Mg) solid solution and Al_3Mg_2 occurs producing LiH, AlB_2, $MgAlB_4$ and H_2. Finally, LiH reacts with AlB_2 to form LiAl, B and H_2. The overall reaction process can be described by the following reactions:

$$\begin{aligned}
6LiBH_4+Mg(AlH_4)_2 &\xrightarrow{70\text{-}150\ ^\circ C} 6LiBH_4+MgH_2+2Al+3H_2 \\
&\xrightarrow{250\text{-}300\ ^\circ C} 6LiBH_4+\frac{1}{2}Al(Mg)+\frac{1}{2}Al_3Mg_2+4H_2 \\
&\xrightarrow{300\text{-}420\ ^\circ C} 6LiH+MgAlB_4+AlB_2+13H_2 \\
&\xrightarrow{420\text{-}500\ ^\circ C} 5LiH+MgAlB_4+LiAl+2B+\frac{27}{2}H_2
\end{aligned} \tag{4}$$

Here, it is deduced that B should exist in the final dehydrogenation product according to the chemical balance; however, it is rather hard

RSC Advances Accepted Manuscript

This journal is © The Royal Society of Chemistry 2012

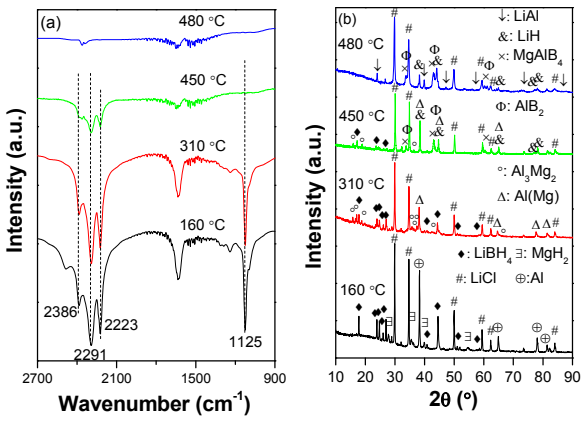

Fig. 6 FTIR spectra (a) and XRD patterns (b) of the $6LiBH_4$-$Mg(AlH_4)_2$-2LiCl composite dehydrogenated at different temperatures.

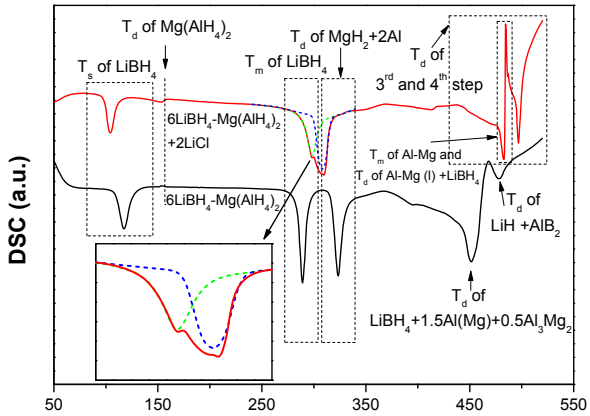

Fig. 7 DSC curves of the $6LiBH_4$-$Mg(AlH_4)_2$ composite with and without LiCl. The inset shows an enlarged view of the overlapping peaks.

to detect only by XRD due to its poor crystallinity. Theoretically, the dehydrogenation amounts of the four steps of equation (4) were calculated to be 2.8, 0.9, 8.3 and 0.4 wt%, respectively, which offers a total dehydrogenation capacity of 12.4 wt%. This is in good agreement with the experimental results shown in Fig. 3 and Table 1.

Fig. 6 shows the FTIR spectra and XRD patterns of the dehydrogenated $6LiBH_4$-$Mg(AlH_4)_2$-2LiCl composite at different temperatures. It can be observed that the LiCl remained nearly constant throughout the dehydrogenation process, suggesting that it did not take part in the dehydrogenation reaction. Moreover, the structural changes of the $6LiBH_4$-$Mg(AlH_4)_2$-2LiCl composite are very similar to those of the $6LiBH_4$-$Mg(AlH_4)_2$ composite upon heating, representing the occurrence of identical chemical events during dehydrogenation.

It should be noted that in the present study, the dehydrogenation pathway is slightly different from a previous report,[19] in which only the first three hydrogen desorption steps occurred, and the reaction between LiH and AlB_2 did not take place in the temperature range of 25-500 °C. This is potentially due to the difference in the hydrogen pressure within the reactor after dehydrogenation. As a hydrogen desorption reaction, the reaction temperature of LiH and AlB_2 is closely related to the hydrogen pressure. Therefore, we believe that the different hydrogen pressure inside the reactor after dehydrogenation should be responsible for the different dehydrogenation pathways.

To elucidate the role of LiCl in lowering the temperature of the second dehydrogenation step and raising the temperature of the third dehydrogenation step of the $6LiBH_4$-$Mg(AlH_4)_2$ composite, the thermodynamic and kinetic parameters of the dehydrogenation of the $6LiBH_4$-$Mg(AlH_4)_2$ and $6LiBH_4$-$Mg(AlH_4)_2$-2LiCl composites were examined and compared. Fig. 7 shows the DSC curves of the $6LiBH_4$-$Mg(AlH_4)_2$ and $6LiBH_4$-$Mg(AlH_4)_2$-2LiCl composites at a heating rate of 10 °C/min. Six heat-flow peaks were observed one after another in the DSC curve of the $6LiBH_4$-$Mg(AlH_4)_2$ composite upon heating, representing a complicated heat effect during dehydrogenation. The endothermic peak at 100-140 °C should be attributed to the phase transformation of $LiBH_4$ (Pnma to $P6_3mc$) according to a previous report.[14] At 150-170 °C, the weak exothermic peak corresponds to the decomposition of $Mg(AlH_4)_2$ to of $LiBH_4$ moved to a higher temperature with respect to the $6LiBH_4$-$Mg(AlH_4)_2$ composite, which induces an overlap with the chemical reaction process of MgH_2 and Al (the inset of Fig. 7). It was reported that $LiBH_4$ and LiCl could form a solid solution of $LiBH_4$(Cl) and stabilise the $P6_3mc$ phase of $LiBH_4$,[30] which should be the most important reason for the lowered phase transformation temperature and elevated melting temperature of $LiBH_4$. In addition, it is noted that the endothermic peak corresponding to dehydrogenation by reacting MgH_2 with Al was moved to a lower temperature. However, there is an apparent shift to a higher temperature for the heat flow peaks of the third and fourth dehydrogenation steps. Moreover, this step can be divided into the following two overlapping parts: a wide endothermic peak at the temperature range of 370-500 °C and a severe fluctuation at 450-470 °C. According to equation (4), the wide endothermic peak corresponds to the solid-state reaction between $LiBH_4$, the Al(Mg) solid solution and Al_3Mg_2 to finally form LiAl and AlB_2. The sharp endothermic peak in the severe fluctuation can be attributed to the melting of the Al-Mg phases because this process occurs at 450 °C.[27] The following sharp exothermic peak is then believed to be the reaction between the liquid Al-Mg phase and $LiBH_4$. A similar phenomenon was also observed in the DSC measurement of pristine $LiAlH_4$.[31] These results agree well with the TPD and volumetric release experiments. More interestingly, by normalising the DSC curves, it is found that the integrated intensities of the heat-flow peaks were roughly identical for the $6LiBH_4$-$Mg(AlH_4)_2$ and $6LiBH_4$-$Mg(AlH_4)_2$-2LiCl composites, suggesting that the presence of LiCl does not appreciably change the thermodynamic properties of the dehydrogenation reaction of the $6LiBH_4$-$Mg(AlH_4)_2$ composite.

The apparent activation energy (E_a) of the dehydrogenation reaction was determined by Kissinger's method using the following equation:[32]

$$\ln\left(\frac{\beta}{T_m^2}\right) = -\frac{E_a}{RT_m} + C \qquad (5)$$

in which β is the heating rate, T_m is the absolute temperature for the maximum reaction rate, and R is the gas constant. In this case, the temperatures corresponding to the maximum reaction rate (T_m) were

RSC Advances Accepted Manuscript

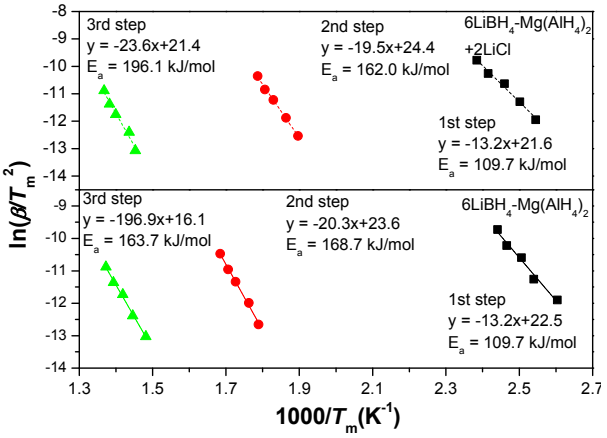

Fig. 8 Kissinger plots of the $6LiBH_4$-$Mg(AlH_4)_2$ composite (a) and the $6LiBH_4$-$Mg(AlH_4)_2$-2LiCl composite (b).

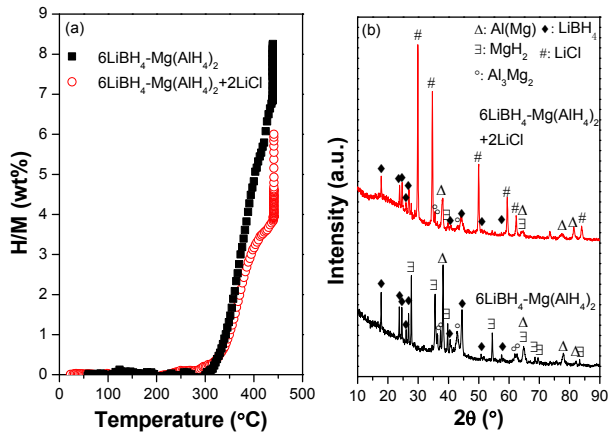

Fig. 9 (a) Hydrogenation curves of dehydrogenated $6LiBH_4$-$Mg(AlH_4)_2$ with and without LiCl under 100 atm of hydrogen pressure; (b) XRD patterns of the hydrogenated samples.

extracted by differentiating the volumetric release curves at 1-10 ºC/min. Fig. 8 demonstrates the Kissinger plots of the $6LiBH_4$-$Mg(AlH_4)_2$ and $6LiBH_4$-$Mg(AlH_4)_2$-2LiCl composites. Because the amounts of hydrogen desorbed from the fourth dehydrogenation steps are quite small, only the apparent activation energies (E_a) of the first three dehydrogenation steps were calculated, which are 109.7, 168.7 and 163.7 kJ/mol for the $6LiBH_4$-$Mg(AlH_4)_2$ composite and 109.7, 162.0 and 196.1 kJ/mol for the $6LiBH_4$-$Mg(AlH_4)_2$-2LiCl composite. It is clear that, for the $6LiBH_4$-$Mg(AlH_4)_2$-2LiCl composite, the E_a value of the second dehydrogenation step was reduced while it was enlarged for the third dehydrogenation step in comparison with the $6LiBH_4$-$Mg(AlH_4)_2$ composite. The change in the activation energy can reasonably be assumed to be responsible for the change in the dehydrogenation temperatures with the presence of LiCl. The lowered dehydrogenation temperature for the reaction between MgH_2 and Al, which corresponds to the second dehydrogenation step, is likely to be ascribed to the substitution of the Cl^- anion for the H^- anion in MgH_2 as reported previously,[33] which decreases the energy for the removal of H_2. Moreover, the dehydrogenation reaction between $LiBH_4$ and the Al-Mg phases should occur on the surface of the Al-Mg phases because the $LiBH_4$ melts into the liquid phase above 280 ºC. The presence of LiCl blocks the contact of $LiBH_4$ and the Al-Mg, which subsequently induces a high dehydrogenation temperature. A similar phenomenon was also observed in the hydrogenation of the Li_3N/Mg_3N_2 composites.[34] Such a conclusion was further proved by the appearance of a sharp dehydrogenation peak in the TPD curve of the $6LiBH_4$-$Mg(AlH_4)_2$-2LiCl composite at 446 ºC, which represents a fast dehydrogenation rate due to the improved contact between the Al-Mg phases and $LiBH_4$ caused by the melting of the Al-Mg phases at such a temperature.

The effects of the LiCl on the hydrogen storage reversibility of the $6LiBH_4$-$Mg(AlH_4)_2$ composite were further investigated by re-hydrogenating the dehydrogenated products under 100 atm of hydrogen pressure. Fig. 9a shows the hydrogenation curves of the dehydrogenated $6LiBH_4$-$Mg(AlH_4)_2$ and $6LiBH_4$-$Mg(AlH_4)_2$-2LiCl composites as a function of temperature. It can be observed that the dehydrogenated samples started absorbing hydrogen at approximately 300 °C, and the hydrogen uptakes amounted to 8.3 and 6.0 wt% for the $6LiBH_4$-$Mg(AlH_4)_2$ and $6LiBH_4$-$Mg(AlH_4)_2$-2LiCl composites while dwelling at 450 °C for 24 hours, which correspond to 70% and 69% of the respective dehydrogenation amounts, representing an analogous hydrogenation behaviour. In addition, it should be noted that only partial hydrogen was recharged into the dehydrogenated samples potentially due to the insufficient hydrogen pressure applied in the present study. Fig. 9b presents the XRD patterns of the hydrogenated samples with and without LiCl. The characteristic reflections of $LiBH_4$, MgH_2, Al(Mg) and Al_3Mg_2 were detected in the two hydrogenated samples. In addition, the LiCl phase persisted in the XRD profile of the hydrogenated $6LiBH_4$-$Mg(AlH_4)_2$-2LiCl sample. As a result, we deduce that the following reactions took place during hydrogenation in the present study:

$$\mathrm{LiAl}+2\mathrm{B}+\frac{1}{2}\mathrm{H_2}\rightarrow\mathrm{LiH}+\mathrm{AlB_2} \quad (6)$$

$$5\mathrm{LiH}+\mathrm{MgAlB_4}+\mathrm{LiAl}+2\mathrm{B}+\frac{19}{2}\mathrm{H_2}\rightarrow 6\mathrm{LiBH_4}+\frac{1}{2}\mathrm{Al_3Mg_2}+\frac{1}{2}\mathrm{Al(Mg)} \quad (7)$$

$$\frac{1}{2}\mathrm{Al_3Mg_2}+\frac{1}{2}\mathrm{Al(Mg)}+\mathrm{H_2}\rightarrow\mathrm{MgH_2}+2\mathrm{Al} \quad (8)$$

It was reported that Al_3Mg_2 and Al(Mg) were fully hydrogenated at 210 °C and 100 atm of hydrogen pressure.[27] However, in the present study, the hydrogenation temperature was as high as 450 ºC, which possibly induces the occurrence of a partial reversal of reaction (8). This is responsible for the insufficient hydrogenation as mentioned above. Moreover, it should be noted that approximately 75% of the reversible capacity was achieved for the $6LiBH_4$-$Mg(AlH_4)_2$ composite when it was only heated to 450 °C, while the reversible capacity was found to be only 56% for the $6LiBH_4$-$Mg(AlH_4)_2$-2LiCl composite under identical conditions by calculating the extent of reaction. These results indicate that the presence of LiCl in the $6LiBH_4$-$Mg(AlH_4)_2$ composite not only decreases the available hydrogen capacity but also slows down the hydrogenation rate, which is rather unfavourable for practical applications.

Conclusions

The effects of NaCl and LiCl on the hydrogen storage behaviours of a $6LiBH_4$-$Mg(AlH_4)_2$ composite were systematically investigated. It

RSC Advances Accepted Manuscript

 This journal is © The Royal Society of Chemistry 2012

was determined that the presence of NaCl and LiCl significantly reduced the practical hydrogen storage capacity because no hydrogen is included in these two compounds. In addition, NaCl could react with $LiBH_4$ to form LiCl and $NaBH_4$ during ball milling, which changes the chemical composition of the $6LiBH_4$-$Mg(AlH_4)_2$-2NaCl composite. However, the presence of LiCl changed the apparent activation energy of the dehydrogenation reaction of the $6LiBH_4$-$Mg(AlH_4)_2$ composite even though it did not participate in the dehydrogenation reaction. This is the most important reason for the change in the dehydrogenation temperature of the $6LiBH_4$-$Mg(AlH_4)_2$-2LiCl composite. We therefore believe that the presence of the by-products NaCl and LiCl, which were produced during the synthesis of $Mg(AlH_4)_2$, is quite unfavourable for practical applications.

Acknowledgements

We gratefully acknowledge the financial support received from the National Natural Science Foundation of China (51171170, 51222101, 51025102), the Research Fund for the Doctoral Program of Higher Education of China (20130101110080, 20130101130007), the Program for Innovative Research Team in the University of Ministry of Education of China (IRT13037), and the Fundamental Research Funds for the Central Universities (2014XZZX003-08).

Notes and references

[a]State Key Laboratory of Silicon Materials, Key Laboratory of Advanced Materials and Applications for Batteries of Zhejiang Province and Department of Materials Science and Engineering, Zhejiang University, Hangzhou 310027, People's Republic of China. Tel/Fax: +86 571 87952615, E-mail: mselyf@zju.edu.cn
[b]Shanghai Key Laboratory of Modern Metallurgy and Materials Processing, Shanghai University, Shanghai 200072, China.

1 L. Schlapbach, and A. Züttel, *Nature*, 2001, **414**, 353-358.
2 P. M. Grant, *Nature*, 2003, **424**, 129-130.
3 S. Orimo, Y. Nakamori, J. R. Eliseo, A. Züttel, and C. M. Jensen, *Chem. Rev.*, 2007, **107**, 4111-4132.
4 B. Bogdanović, U. Eberle, M. Felderhoff and F. Schüth, *Scripta Mater.*, 2007, **56**, 813-816.
5 B. Bogdanović and M. Schwickardi, *J. Alloys Compd.* 1997, **253**, 1-9.
6 B. Bogdanović, R. A. Brand, A. Marjanović, M. Schwickardi, J. Tölle, *J. Alloys Compd.* 2000, **302**, 36-58.
7 Targets for Onboard Hydrogen Storage for Light-Duty Fuel Cell Vehicles, US Department of Energy, http://www.energy.gov/sites/prod/files/2014/03/f12/targets_onboard_hydro_storage.pdf. Accessed 10 October 2009.
8 U. Eberle, M. Felderhoff and F. Schüth, *Angew. Chem. Int. Edit.*, 2009, **48**, 6608-6630.
9 M. Fichtner, and O. Fuhr, *J. Alloys Compd.*, 2002, **345**, 286-296.
10 Y. P. Pang, Y. F. Liu, X. Zhang, M. X. Gao, and H. G. Pan, *Int. J. Hydrogen Energy*, 2013, **38**, 13343-13351.
11 Y. P. Pang, Y. F. Liu, M. X. Gao, L. Z. Ouyang, J. W. Liu, H. Wang, M. Zhu and H. G. Pan, *Nat. Commun.*, 2014, **5**, 4519
12 A. Züttel, S. Rentsch, P. Fischer, P. Wenger, P. Sudan, P. Mauron and C. Emmenegger, *J. Alloys Compd.*, 2003, **356**, 515-520.
13 P. Mauron, F. Buchter, O. Friedrichs, A. Remhof, M. Bielmann, C. N. Zwicky and A. Züttel, *J. Phys. Chem. B*, 2008, **112**, 906–910.
14 A. Züttel, A. Borgschulte, and S. Orimo, *Scripta Mater.*, 2007, **56**, 823-828.
15 J. J. Vajo, S. L. Skeith and F. Mertens, *J. Phys. Chem. B*, 2005, **109**, 3719-3722.
16 J. Yang, A. Sudik and C. Wolverton, *J. Phys. Chem. C*, 2007, **111**, 19134-19140.
17 S. A. Jin, J. H. Shim, Y. W. Cho, K. W. Yi, O. Zabara and M. Fichtner, Scripta Mater., 2008, **58**, 963-965.
18 Q. Shi, X. Yu, R. Feidenhans'l, and T. Vegge, *J. Phys. Chem. C*, 2008, **112**, 18244-18248.
19 D. M. Liu. Q. Q. Liu, T. Z. Si, Q. A. Zhang, F. Fang, D. L. Sun, L. Z. Ouyang and M. Zhu, *Chem. Commun.*, 2011, **47**, 5741-5743.
20 R. Mohtadi, P. Sivasubramanian, S. J. Hwang, A. Stonwe, J. Gray, T. Matsunaga and R. Zidan, *Int. J. Hydrogen Energy*, 2012, **37**, 2388-2396.
21 J. F. Mao, X. B. Yu, Z. P. Guo, C. K. Poh. H. K. Liu, Z. Wu, J. Ni, *J. Phys. Chem. C*, 2009, **113**, 10813-10818.
22 Y. J. Yang, M. X. Gao, Y. F. Liu, J. H. Wang, J. Gu, H. G. Pan and Z. X. Guo, *Int. J. Hydrogen Energy*, 2012, **37**, 10733-10742.
23 Y. F. Liu, Y. J. Yang, Y. F. Zhou, Y. Zhang, M. X. Gao and H. G. Pan, *Int. J. Hydrogen Energy*, 2012, **37**, 17137-17145.
24 S. Singh and S. Eijt, *Phys. Rev. B*, 2008, **78**, 224110.
25 Y. F. Liu, F. H. Wang, Y. H. Cao, M. X. Gao, H. G. Pan and Q. D. Wang, *Energy Environ. Sci.*, 2010, **3**, 645-653.
26 B. Li, Y. F. Liu, C. Li, M. X. Gao and H. G. Pan, *J. Mater. Chem. A*, 2014, **2**, 3155-3162.
27 Y. F. Liu, Y. P. Pang, X. Zhang, Y. F. Zhou, M. X. Gao and H. G. Pan, *Int. J. Hydrogen Energy*, 2012, **37**, 18148-18154.
28 D. R. Lide, *CRC Handbook of Chemistry and Physics,* CRC Press/Taylor and Francis, Boca Raton, FL.
29 Y. P. Pang, Y. F. Liu, X. Zhang, M. X. Gao and H. G. Pan, *Int. J. Hydrogen Energy*, 2013, **38**, 1460-1468.
30 L. M. Arnbjerg, D. B. Ravnsbæk, Y. Filinchuk, R. T. Vang, Y. Cerenius, F. Besenbacher, J.-E. Jørgensen, H. J. Jakobsen and T. R. Jensen, *Chem. Mater.*, 2009, **21**, 5772-5782.
31 F. Zhai, P. Li, A. Sun, S. Wu, Q. Wan, W. Zhang, Y. Li, L. Cui and X. Qu, *J. Phys. Chem. C*, 2012, **116**, 11939-11945.
32 H. E. Kissinger, *Anal. Chem.*, 1957, **29**, 1702-1706.
33 J. Wang, Y. Du, L. Sun and X. Li, *Int. J. Hydrogen Energy*, 2014, **39**, 877-883.
34 B. Li, Y. F. Liu, Y. Zhang, M. X. Gao and H. G. Pan, *J. Phys. Chem. C*, 2012, **116**, 13551-13558.

RSC Advances Accepted Manuscript